ISSN 0005-1179, Automation and Remote Control, 2014, Vol. 75, No. 9, pp. 1655–1664. © Pleiades Publishing, Ltd., 2014.
Original Russian Text © A.P. Kirsanov, 2014, published in Avtomatika i Telemekhanika, 2014, No. 9, pp. 144–155.



# Covert Motion Trajectories for an Airborne Object in the Detection Zone of an Onboard Doppler Radar Station

**A. P. Kirsanov**

*National Research University Higher School of Economics, Moscow, Russia*
*e-mail: ki@hse.ru*

Received August 30, 2013

**Abstract**—We study the characteristic features of the detection zone for an onboard radar station for an early radar detection system operating in the impulse–Doppler mode. We show that due to these features, there exist covert trajectories such that objects flying along such trajectories are not detected by this onboard radar station. We derive differential equations that define covert trajectories, find various forms of covert trajectories, and study their properties.

**DOI:** 10.1134/S0005117914090112

## 1. INTRODUCTION

Aviation early radar detection systems (ERDS), which in Russian terminology are called aviation complexes of radar surveillance and coaching (AC RSC), are complex specialized aviation-based informational and control systems that are able to rapidly, constantly (year-round and round-the-clock), and independently of weather conditions provide data regarding the situation in large regions of air space, aquatic areas, and land surface [1, 2]. Such multifunctional systems are usually developed as double purpose systems, which means that they can be used both for civilian and military purposes: reconstructing and increasing the radar field in zones of military conflict, natural hazards, and industrial disasters; control over air traffic around airport hubs; surveillance over navigation and escorting vessels on large aquatic areas etc.

The main purpose of ERDS systems that differentiates them from land-based radar systems is to detect and track stealthy low-flying airborne objects (AO) against the background of reflections from the surface of the Earth. In such conditions, it is possible to detect an AO due to the difference in radial velocities of the AO and the surface with respect to the onboard radar station in the ERDS system. To use this effect, onboard radar station uses a coherent impulse mode with high frequency of repeating the impulses and Doppler filtering for the pack of coherent signals reflected from the background and the AO [1–3]. In what follows we call radar stations operating in this mode impulse–Doppler radar stations (IDRS).

An important property of the detection zone of an IDRS is that at every point of this zone there exist directions of AO motion for which radial components of the AO and underlying surface velocities coincide, so AO cannot be detected by radar stations with Doppler signal filtering. This means that in the detection zone one can construct covert trajectories, i.e., such trajectories that an object flying along them remains undetected by the onboard radar station.

In this work, we consider the properties of the detection zone of an IRDS operating in Doppler filtering mode, derive differential equations that define covert trajectories, find and describe various forms of covert trajectories.

## 2. FEATURES OF THE DETECTION ZONE FOR LOW-FLYING AIRBORNE OBJECTS IN A DOPPLER RADAR STATION ERDS SYSTEM

In the Doppler operation mode of an onboard radar station, reflected signals whose frequencies are close to the average frequency of a signal reflected from the Earth's surface in the direction of the principal ray of the antenna's directional response remain undetected since the radar station's receiver has a special filter (resection filter) [1–3]. The frequency of the reflected signal depends on the frequency of the emitted signal and the Doppler shift caused by the motion of the airplane on which the radar station is installed. Doppler shift of the frequency is proportional to the radial component of the relative velocity of the illuminated object (target or underlying surface), i.e., projection of the object's relative velocity on the line of sight "radar station—object" in the coordinate system related to the moving radar station (see Fig. 1). The origin of this moving coordinate system $z_1Oz_2$ is located at the ERDS airplane, and the $Oz_1$ axis is directed along the velocity vector of the ERDS airplane.

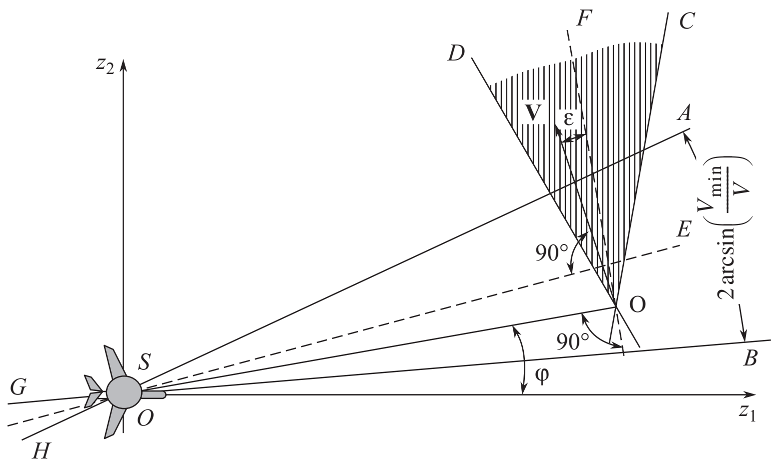


**Fig. 1.** Scheme of resection sectors and SIMD.

Thus, all reflecting objects for which the radial component of the relative velocity $V_{\rm rel}^R$ differs from the radial component of the underlying surface velocity $V_{\rm us}^R$ with respect to the onboard radar station by at most some predefined value $V_{\min}$, i.e., objects that satisfy inequality

$$\left|V_{\rm rel}^R - V_{\rm us}^R\right| < V_{\min}, \tag{1}$$

are invisible for the radar station. The value $V_{\min}$ is a parameter of the resection filter and is chosen depending on the bandwidth of the reflected signal's spectrum. Velocities of the flying object $\mathbf{V}_{\rm rel}$ and the underlying surface $\mathbf{V}_{\rm us}$ with respect to the ERDS airplane can be expressed via velocity vectors of the AO $\mathbf{V}$ and the carrier (ERDS airplane) $\mathbf{V}_{\rm c}$ in some Earth-based coordinate system with the following formulas: $\mathbf{V}_{\rm rel} = \mathbf{V} - \mathbf{V}_{\rm c}$, $\mathbf{V}_{\rm us} = -\mathbf{V}_{\rm c}$. Therefore, $\mathbf{V}_{\rm rel} - \mathbf{V}_{\rm us} = \mathbf{V}$.

We denote by $(\mathbf{x}, \mathbf{y})$ the scalar product of vectors $\mathbf{x}$ and $\mathbf{y}$. Then the radial component $V_{\rm rel}^R - V_{\rm us}^R$ of vector $\mathbf{V}_{\rm rel} - \mathbf{V}_{\rm us}$ can be represented as the scalar product $V_{\rm rel}^R - V_{\rm us}^R = V^R = \left(\mathbf{V}, \frac{\mathbf{z}}{|\mathbf{z}|}\right)$, where $\mathbf{z} = \begin{pmatrix} z_1 \\ z_2 \end{pmatrix}$ is the vector that defines AO position in the coordinate system $z_1Oz_2$ related to the onboard radar station (Fig. 1), and $|\mathbf{z}|$ is the length of vector $\mathbf{z}$. Due to this representation, inequality (1) can be transformed as

$$|(\mathbf{V}, \mathbf{z})| \leqslant V_{\min} |\mathbf{z}| . \tag{2}$$

Expression (2) characterizes the AO invisibility condition due to its falling into the resection zone expressed in relative coordinates and the AO velocity vector in the Earth-based coordinate system.

Inequality (2) implies that resection zones have the form of sectors. Boundaries of resection sectors are shown on Fig. 1 with straight lines $AH$ and $BG$ intersecting at the location of the onboard radar station on the ERDS airplane (point $S$ on Fig. 1). Condition (2) implies that the common bisecting line of resection sectors is always perpendicular to the direction of AO flight, and the angular size $\alpha$ of each sector is given by

$$\alpha = 2\arcsin\frac{V_{\min}}{V}, \tag{3}$$

where $V$ is the AO flight velocity.

Condition (2) implies that at every point of the detection zone an AO has a sector of directions such that the onboard IDRS of the ERDS airplane will not detect it as long as it moves in these directions. In what follows we call this sector the sector of invisible motion directions (SIMD) of the flying object. SIMD orientation is defined by AO location, and the orientation of resection sectors is defined by the AO motion direction (see Fig. 1).

The apex of SIMD is located at the current AO location (point O on Fig. 1). The bisecting line (symmetry axis) O$F$ of the sector of invisible motion directions is perpendicular to the "ERDS airplane—AO" line of sight $S$O, and the velocity vector $\mathbf{V}$ of the flying object is perpendicular to the bisecting line $SE$ of the resection sector. Therefore, the angle $\mathbf{V}$O$F$ between velocity vector $\mathbf{V}$ and bisecting line of the SIMD equals the O$SE$ angle between the line of sight $S$O and bisecting line of the resection sector. In particular, if the AO velocity vector coincides with the SIMD boundary, it means that the AO is located at the boundary of the resection zone. Our reasoning has two different implications now. First, the angular size of the sector of invisible motion directions coincides with the angular size of the resection sector defined by formula (3); second, when the target's velocity vector (in the Earth coordinate system) falls into the SIMD it is equivalent to the AO being located in the resection zone.

Now (3) implies that the smaller is the velocity of the flying object, the wider is the corresponding SIMD and the more options there are for covert maneuvering in the detection zone of an onboard radar station of an ERDS airplane. The characteristic features of the detection zone for a Doppler radar station have been considered in more detail in [4–6].

## 3. EQUATIONS OF COVERT MOTION TRAJECTORIES OF AN AO IN THE IDRS DETECTION ZONE

AO motion occurs in the resection sector, and an AO is not detected by the onboard radar station of the ERDS airplane if inequality (2) holds. We should note that if the velocity vector of the flying object $\mathbf{V}$ satisfies inequality (2), this inequality is also satisfied for the opposite vector $(-\mathbf{V})$. Therefore, there are two options for the AO's covert motion. In the first possibility, the flying object during its motion along a covert trajectory "rotates" the onboard radar station—AO line of sight counterclockwise. According to Fig. 1, AO velocity vector $\mathbf{V}$ is rotated by angle $\frac{\pi}{2} + \varepsilon$ with respect to the onboard radar station—AO line of sight (the bisecting line of the SIMD is rotated by $\frac{\pi}{2}$ with respect to the line of sight, and the AO velocity vector is rotated by angle $\varepsilon$ with respect to the bisecting line) and is given by expression

$$\mathbf{V} = \begin{pmatrix} v \times \cos\left(\varphi + \varepsilon + \dfrac{\pi}{2}\right) \\ v \times \sin\left(\varphi + \varepsilon + \dfrac{\pi}{2}\right) \end{pmatrix}. \tag{4}$$

We denote by $\varphi$ the angle between the vector $\mathbf{z}$ and axis $Oz_1$ counted counterclockwise.

In the second possibility, covert flying motion occurs with the opposite velocity vector

$$-\mathbf{V} = \begin{pmatrix} v \times \cos\left(\varphi + \varepsilon - \dfrac{\pi}{2}\right) \\ v \times \sin\left(\varphi + \varepsilon - \dfrac{\pi}{2}\right) \end{pmatrix}$$

and the line of sight rotates clockwise.

As we will see below, families of covert trajectories corresponding to these two possibilities are symmetric with respect to the horizontal axis $Oz_1$ related to the onboard radar station coordinate system. Due to this symmetry, we will only consider in detail the first of these two covert motion possibilities.

In what follows we consider the covert motion of an AO with constant velocity $v = |\mathbf{V}|$ and constant angle $\varepsilon$ between the AO velocity vector and the SIMD bisecting line. We assume that the ERDS airplane moves along a straight line with constant velocity $v_{\mathrm{c}} = |\mathbf{V}_{\mathrm{c}}|$.

AO motion in the coordinate system related to the Doppler radar station of the ERDS airplane is defined by equation

$$\dot{\mathbf{z}} = \mathbf{V} - \mathbf{V}_{\mathrm{c}}. \tag{5}$$

To simplify the analytic expressions, we use an Earth-based coordinate system where the velocity vector of the ERDS airplane has the form $\mathbf{V}_{\mathrm{c}} = \begin{pmatrix} v_{\mathrm{c}} \\ 0 \end{pmatrix}$. Substituting this expression and (4) into (5), we get the AO motion equation in the coordinate system related to the ERDS airplane:

$$\begin{cases} \dot{z}_1 = -v \times \sin(\varphi + \varepsilon) - v_{\mathrm{c}} \\ \dot{z}_2 = v \times \cos(\varphi + \varepsilon). \end{cases} \tag{6}$$

To solve this system of equations, we write it in polar coordinates. We express $\dot{z}_1$ and $\dot{z}_2$ via polar coordinates:

$$\dot{z}_1 = \frac{d}{dt}(\rho \times \cos\varphi) = \dot{\rho} \times \cos\varphi - \dot{\varphi}\rho \times \sin\varphi,$$

$$\dot{z}_2 = \frac{d}{dt}(\rho \times \sin\varphi) = \dot{\rho} \times \sin\varphi + \dot{\varphi}\rho \times \cos\varphi.$$

Substituting these expressions into (6) and resolving the resulting equations with respect to $\dot{\rho}$ and $\dot{\varphi}$, we get the following system:

$$\begin{cases} \dot{\rho} = -v \times \sin\varepsilon - v_{\mathrm{c}} \times \cos\varphi \\ \dot{\varphi} = \dfrac{1}{\rho}(v \times \cos\varepsilon + v_{\mathrm{c}} \times \sin\varphi), \end{cases} \tag{7}$$

which is equivalent to the differential equation

$$\frac{d\rho}{d\varphi} = -\rho\,\frac{v \times \sin\varepsilon + v_{\mathrm{c}} \times \cos\varphi}{v \times \cos\varepsilon + v_{\mathrm{c}} \times \sin\varphi}.$$

This is an equation with separating variables, and its solution has the form

$$\rho = \left|\frac{1}{\mu + \sin\varphi}\right| \times \exp\left(-\frac{v \times \sin\varepsilon}{v_{\mathrm{c}}} \times \int \frac{d\varphi}{\mu + \sin\varphi}\right), \quad \text{where} \quad \mu = \frac{v}{v_{\mathrm{c}}} \times \cos\varepsilon. \tag{8}$$

The differential equation that defines the second family of covert trajectories, for which the onboard radar station—AO line of sight rotates clockwise, has the form

$$\frac{d\rho}{d\varphi} = \rho\,\frac{v \times \sin\varepsilon - v_{\mathrm{c}} \times \cos\varphi}{-v \times \cos\varepsilon + v_{\mathrm{c}} \times \sin\varphi},$$

and its solution is given by

$$\rho = \left|\frac{1}{\mu - \sin\varphi}\right| \times \exp\left(-\frac{v \times \sin\varepsilon}{v_{\mathrm{c}}} \times \int \frac{d\varphi}{\mu - \sin\varphi}\right). \qquad (9)$$

These expressions let us find covert trajectories of AO motion for various relations of velocities $v$, $v_{\mathrm{c}}$, and the angle $\varepsilon$ by which the AO velocity vector deviates from the SIMD bisecting line.

## 4. COVERT MOTION TRAJECTORIES FOR THE FLYING OBJECT. ORTHOGONAL VERSION

Trajectories of covert approach are based on expressions (8) and (9). We remind that they have been obtained under the assumption that the IDRS moves along a straight line with constant velocity $v_{\mathrm{c}}$.

As we have already noted, covertness of AO motion follows since the AO velocity vector is located in the SIMD. The location and orientation of the SIMD depend on the IDRS (ERDS airplane) and AO motion parameters, which are usually only known with certain errors. Therefore, covert motion direction will also be determined with errors. Besides, the exact value $V_{\min}$ of the minimal admissible radial velocity of the Doppler radar station is unknown. Therefore, in order to reliably ensure that motion is covert the flying object should stay in the center of the SIMD, i.e., it should have the AO velocity vector coincide with the SIMD bisecting line. Trajectories that result when the targeting AO is located at the center of the SIMD are called orthogonal since in this case the AO velocity vector is orthogonal to the radar station—AO line of sight ($\varepsilon = 0$).

To get a solution for the family of orthogonal covert trajectories in polar coordinates, it suffices to let $\varepsilon = 0$ in (8). Expression (8) defines not a single trajectory but rather an entire family of trajectories due to the indeterminate integral in the right-hand side exponent of (8). Equation of the trajectory that passes through the point $(\rho_0, \varphi_0)$ has the form

$$\rho = \frac{c_0}{\sin\varphi + \mu_0} = \rho_0 \frac{\sin\varphi_0 + \mu_0}{\sin\varphi + \mu_0}, \quad \text{where} \quad \mu_0 = \frac{v}{v_{\mathrm{c}}}. \qquad (10)$$

This equation defines conical sections in polar coordinates. Depending on the relation between velocities $v$ and $v_{\mathrm{c}}$, sections may be either parabolas, ellipses, or hyperbolas. One focal point of these conical sections is located at the origin of the moving coordinate system, i.e., at the location of the onboard radar station on an ERDS airplane. This result implies an interesting analogy to the motion of planets in a central gravitational field. The properties of invisible trajectories that we have listed are basically Kepler's first law [7]. Moreover, covert trajectories also satisfy Kepler's second law, which says that the sectoral velocity (rate of change for the area spanned by the radius vector) of planets as they move along their trajectories remains constant. Figure 2 illustrates Kepler's second law. Any two sectors O$AB$ and O$CD$ spanned by the radius vector of an AO moving along an elliptic trajectory over equal time intervals have the same area $S$.

Sectoral velocity is given by the following expression from [7]: $\dot{s} = \rho^2\dot{\varphi}$.

To check that Kepler's second law indeed holds it suffices to substitute in this formula an expression for $\dot{\varphi}$ from (7) and take (10) into account:

$$\dot{s} = \rho^2\dot{\varphi} = v_{\mathrm{c}}\rho(\sin\varphi + v/v_{\mathrm{c}}) = v_{\mathrm{c}}c_0 = \text{const}.$$

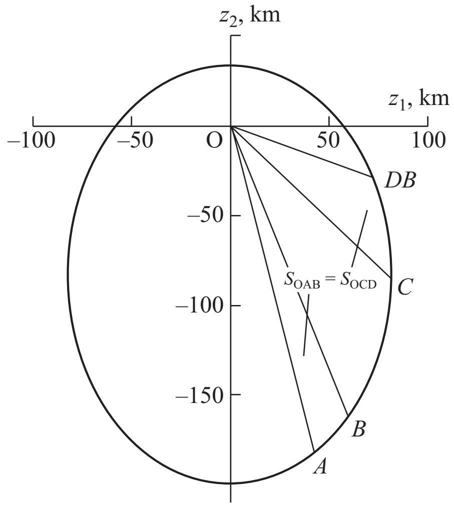


**Fig. 2.** Constant sectoral velocity.

Since sectoral velocity is constant, we can use it to find the time of motion of the AO along covert trajectories from one point to another and to find the moment when we can begin covert motion in the desired direction.

**Elliptical covert trajectories.** Consider the case when velocity $v$ of an AO flying along a covert trajectory in the detection zone of a moving Doppler onboard radar station exceeds the velocity $v_c$ with which the onboard radar station itself moves, i.e., $v > v_c$. Substituting $z_1 = \rho \cos \varphi$ and $z_2 = \rho \sin \varphi$ from (10), we get the trajectory equation in a rectangular coordinate system:

$$\frac{z_1^2}{\frac{v_c^2 c_0^2}{v^2 - v_c^2}} + \frac{\left(z_2 + \frac{v_c^2 c_0^2}{v^2 - v_c^2}\right)^2}{\frac{v_c^2 v^2 c_0^2}{(v^2 - v_c^2)^2}} = 1, \quad \text{where} \quad c_0 = \rho_0(\sin \varphi_0 + v/v_c). \tag{11}$$

This equation defines a family of ellipses with the following semiaxes:

$$a = \frac{v_c c_0}{\sqrt{v^2 - v_c^2}}, \quad b = \frac{v_c v\, c_0}{v^2 - v_c^2},$$

where $b > a$ and, consequently, the ellipse is elongated along the $Oz_2$ axis. One focal point of each ellipse from family (11) is located at the origin (i.e., at the location of the onboard radar station). An elliptic trajectory of covert motion in the coordinate system $z_1 O z_2$ related to the ERDS airplane is shown on Fig. 3. This trajectory corresponds to the ERDS airplane velocity $v_c = 650$ km/h and flying object velocity $v = 1.2 v_c$. The same trajectory is shown on Fig. 4 in the Earth coordinate system.

The minimal $\rho_{\min e}$ and maximal $\rho_{\max e}$ distances from the origin to the ellipse depend on the value $c_0 = \rho_0(\sin \varphi_0 + v/v_c)$ defined by the initial position of the AO and can be computed as

$$\rho_{\min e} = \frac{v_c c_0}{v + v_c}, \quad \rho_{\max e} = \frac{v_c c_0}{v - v_c},$$

while their ratio is independent of the initial position and is given by

$$\frac{\rho_{\min e}}{\rho_{\max e}} = \frac{v - v_c}{v + v_c}. \tag{12}$$

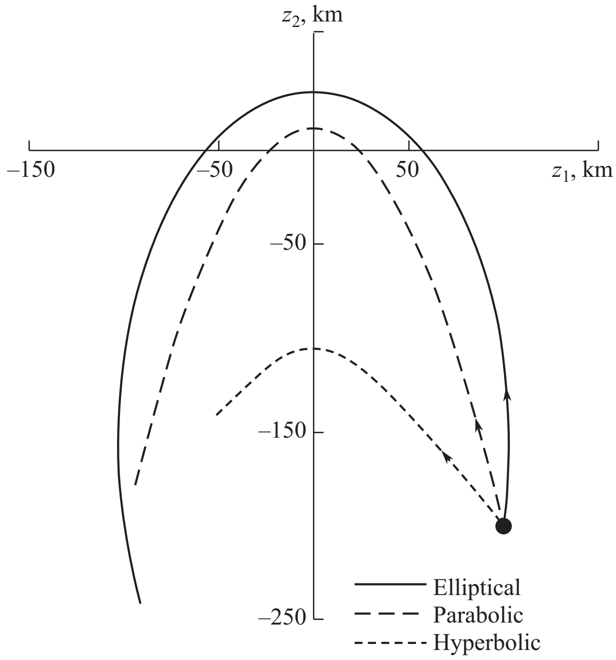


**Fig. 3.** Orthogonal covert trajectories in the coordinate system related to the ERDS airplane.

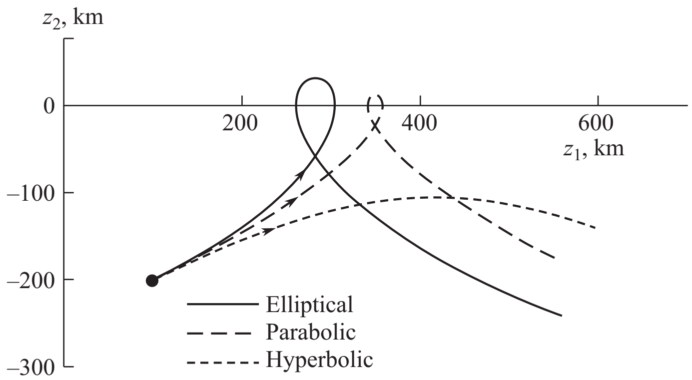


**Fig. 4.** Orthogonal covert trajectories in the Earth-based coordinate system.

Expression (12) implies that the smaller is the difference between the velocities of the AO and the carrier of a Doppler onboard radar station, the closer AO's trajectory passes to the origin for a given initial position of the AO.

Since sectoral velocity is constant (Kepler's second law), when flying along invisible trajectories we can use it to calculate the time $T$ of AO flight from the apocenter (point located at maximal distance from the ellipse's focal point at the origin) of an elliptical trajectory to the pericenter, i.e., the point nearest to the ellipse's focal point where the Doppler onboard radar station is located. It is obvious that when flying from the epicenter to the pericenter the radius vector spans half the area of the ellipse which is equal to $\frac{\pi\times a\times b}{2}$. This fact is expressed by the following equation: $\dot{s}\times T=\frac{\pi\times a\times b}{2}$, where $T$ is the time in question. Since

$$\dot{s}=\frac{v_\mathrm{c}}{2}c_0=\frac{v_\mathrm{c}\rho_{\max}}{2}\left(\frac{v}{v_\mathrm{c}}-1\right),$$

we can find an expression for the time in question:

$$T = \frac{\pi \rho_{\max}}{(v - v_{\rm c})\sqrt{1 - \ v_{\rm c}^2/v^2}} = \frac{\pi c_0 v v_{\rm c}}{(v^2 - v_{\rm c}^2)^{3/2}}. \tag{13}$$

Let us consider a specific example. Let the velocity of IDRS be equal $v_{\rm c} = 650\,{\rm km/h}$, and the velocity of the AO be $v = 1.5v_{\rm c}$. According to (12), we have $\frac{\rho_{\max\,\rm e}}{\rho_{\min\,\rm e}} = \frac{2.5}{0.5} = 5$. This means that if $\rho_{\max\,\rm e} = 200\,{\rm km}$ then the covert trajectory lets one approach the ERDS airplane to a distance of 40 km. The time of AO motion from the apocenter of the elliptical covert trajectory to its pericenter can be computed with (13) and amounts to approximately 31 minutes.

As we have already noted, apart from the trajectories we consider there also exist elliptical covert trajectories that are symmetrical to them with respect to the horizontal coordinate axis.

**Parabolic covert trajectories.** If the velocities of the AO and the carrier of the onboard radar station coincide, i.e., $v = v_{\rm c}$, Eq. (10) can be written as

$$\rho = \rho_0 \frac{\sin\varphi_0 + 1}{\sin\varphi + 1}.$$

This equation defines a parabola passing through the point with polar coordinates $(\rho_0,\ \varphi_0)$ and with focal point at the origin. AO motion along such a trajectory occurs from the fourth quadrant to the third, flying over the origin (the location of the Doppler radar station) counterclockwise. The form of a parabolic covert trajectory in the moving coordinate system is shown on Fig. 3; in the Earth coordinate system the same trajectory is shown on Fig. 4.

The second family of parabolic covert trajectories is given by equation

$$\rho = \frac{c_0}{\sin\varphi - 1},$$

which results from (9) for $\varepsilon = 0$. Trajectories of this family are symmetrical to trajectories from the first family with respect to the $Oz_1$ axis.

There are no parabolic covert trajectories passing through the origin. The minimal distance $\rho_{\min}$ from the origin to the parabola depends on the initial position of the AO and is given by expression

$$\rho_{\min} = \rho_0 \frac{1 + \sin\varphi_0}{2}.$$

Using the fact that sectoral velocity is constant, we can compute the time of AO flight along a parabolic trajectory from the initial point at the right semiplane to the point of the trajectory which is nearest to the origin. For instance, time of flight $T$ along a parabolic trajectory from the point with polar coordinates $(\rho_0,\ \varphi_0)$, $|\varphi_0| < \pi/2$ to the point on the trajectory nearest to the origin is given by the following expression:

$$T = \frac{\rho_0 \cos\varphi_0}{v_{\rm c}} \left( 1 - \frac{\rho_0}{c_0} \sin\varphi_0 - \frac{\rho_0^2 \cos^2\varphi_0}{3c_0^2} \right),$$

where

$$c_0 = \rho_0(1 + \sin\varphi_0).$$

**Hyperbolic covert trajectories.** If the AO velocity is less than the velocity of the onboard radar station carrier, i.e., $v < v_{\rm c}$, expression (10) defines a family of hyperbolas. The same family is also defined by the canonical Eq. (11). Specific hyperbolas can be distinguished from the family by specifying polar coordinates $\rho_{\rm o}$ and $\varphi_{\rm o}$ of a point through which the hyperbola passes. Coordinates $\rho_{\rm o}$ and $\varphi_{\rm o}$ uniquely determine the value $c_0 = \rho_{\rm o}(\sin\varphi_{\rm o} + v/v_{\rm c})$, which is the numerator in (10).

Trajectories for which $c_0 = \rho_0(\sin\varphi_{\rm o} + v/v_{\rm c}) < 0$ are completely contained in the bottom semi-plane bounded by the horizontal coordinate axis. Trajectories for which $c_0 = \rho_0(\sin\varphi_{\rm o} + v/v_{\rm c}) > 0$ pass through all four quadrants of the coordinate plane. The minimal distance from a hyperbolic covert trajectory to the origin (location of the Doppler onboard radar station) for $c_0 > 0$ equals $\frac{c_0}{1+v/v_{\rm c}}$, while for $c_0 < 0$ it is equal to $\frac{c_0}{-1+v/v_{\rm c}}$. Besides, the family of hyperbolic covert trajectories has two special trajectories for which $c_0 = \rho_o(\sin\varphi_{\rm o} + v/v_{\rm c}) = 0$. These are rays coming out of the origin that are defined by equations

$$z_2 = \frac{\mu_0}{\sqrt{1-\mu_0^2}} \times z_1 \quad \text{for} \quad z_1 < 0$$

and

$$z_2 = -\frac{\mu_0}{\sqrt{1-\mu_0^2}} \times z_1 \quad \text{for} \quad z_1 > 0.$$

A useful feature of these trajectories is that motion (approach for one of them) along these trajectories is done along straight line trajectories both in coupled and Earth coordinate system. The approach speed with an ERDS airplane along a straight line trajectory lying in the fourth quadrant is constant and equals $\sqrt{v_{\rm c}^2 - v^2}$. Along this trajectory, the AO gets exactly into the origin. Along another straight line trajectory, the AO can leave the ERDS airplane with the same velocity.

Similar to the two previous cases (parabolic and elliptical), for each covert trajectory there exists a trajectory symmetric to it with respect to the horizontal axis.

## 5. CONCLUSION

Our studies have shown that in the operation of a radar station in an ERDS airplane in impulse–Doppler mode at every point of its detection zone there exists a sector of directions such that AOs remain undetected while moving along them. This lets one form covert motion trajectories for an AO. We have considered orthogonal covert trajectories tangents to which (AO velocity vectors) are orthogonal to the line of sight to the ERDS airplane and are directed along the bisecting line of the invisible motion direction sector. We have established that motion along such orthogonal covert trajectories satisfies the first and second Kepler's laws, i.e., trajectories are conical sections motion along which is done with constant sectoral velocity. We have described a number of characteristic features for such trajectories.

Note that orthogonal trajectories that we have considered in this work are not the only covert trajectories possible. If one abandons orthogonality ($\varepsilon \neq 0$), solution (8) yields a variety of covert trajectories. Analysis of properties for such trajectories may be a subject for further studies.

## REFERENCES

1. Verba, V.S., *Aviatsionnye kompleksy radiolokatsionnogo dozora i navedeniya. Sostoyanie i tendentsii razvitiya* (Aviation Radiolocation Surveillance and Coaching Complexes. State of the Art and Trends in Development), Moscow: Radiotekhnika, 2008.
2. Long, Maurice W., *Airborne Early Radar Warning System Concepts*, SciTech, 2004.
3. *Radar Handbook*, Skolnik, M., Ed., McGraw Hill, 2008, vol. 3, *Radar Devices and Systems.* Translated under the title *Spravochnik po radiolokatsii*, vol. 3, *Radiolokatsionnye ustroistva i sistemy*, Moscow: Sovetskoe Radio, 1976–1979.

4. Gandurin, V.A. and Kirsanov, A.P., Characteristic Features of the Detection Zone for Low-Flying Airborne Objects on a Doppler Radar Station, *Radiotekh.*, 2007, no. 10, pp. 42–46.

5. Gandurin, V.A., Kirsanov, A.P., and Suzanskii, D.N., The Influence of Constructive Features of a Movable Radar Station Suppor on the Configuration of the Radar Field, *Radiotekh.*, 2008, no. 9, pp. 58–62.

6. Verba, V.S., Kirsanov, A.P., and Suzanskii, D.N., Characteristic Features of the Radar Field Configuration for an Aviation Impulse–Doppler Radar Station, *Radiotekh.*, 2010, no. 7, pp. 23–29.

7. Arnol'd, V.I., *Matematicheskie metody klassicheskoi mekhaniki* (Mathematical Methods of Classical Mechanics), Moscow: Editorial URSS, 2003.

*This paper was recommended for publication by E.Ya. Rubinovich, a member of the Editorial Board*